Index of refraction for sodium matter waves traveling in a cold noble-gas medium

Shannon Blanchard, Dave Civello, and Robert C. Forrey
Pennsylvania State University, Berks-Lehigh Valley College, Reading, Pennsylvania 19610
(Received 15 August 2002; published 21 January 2003)

The index of refraction for sodium matter waves traveling in a cold noble-gas medium is calculated as a function of temperature and beam velocity. Resonances and glory oscillations are present in the center-of-mass scattering amplitude and may be seen in the refractive index at very low temperatures. The sensitivity of the calculations to the molecular potential is investigated for the case of argon, and results at 300 K are compared to a recent experiment. Effective range parameters are computed and the attenuation and phase of the matter waves are analyzed as a function of temperature and beam velocity.

DOI: 10.1103/PhysRevA.67.013604 PACS number(s): 03.75.Be

I. INTRODUCTION

The index of refraction for sodium matter waves traveling through various noble gases has been measured using atom interferometry [1–3]. The sensitivity of these measurements has motivated theoretical predictions and may result in refined molecular potentials [4–8]. Glory oscillations and resonances were predicted for the refractive index of sodium matter waves traveling through an argon gas [5,8]. A recent experiment [3] has revealed a full glory oscillation using beam velocities ranging from 700 to 3000 m/s. The experiment also revealed surprising disagreement with theoretical predictions based on molecular potentials that were believed to be reliable. Therefore, it may be necessary to reconsider some of the assumptions that were made in constructing the potentials. It would also be desirable to have a full account of the scattering data for a wide range of parameters (e.g., beam velocity, target gas temperature, variations in the potential, etc) in order to assess the quality of the experimental data or perhaps the applicability of the standard theoretical treatment [7]. We provide such an account for collisions between sodium and argon atoms using potentials constructed from the data of three independent experiments [9–11].

We also investigate the case of slow atomic beams which correspond to matter waves with long de Broglie wavelengths, thus, more pronounced matter wave nature. For a given arrangement of matter wave diffraction, slower beams provide larger diffraction angles, larger enclosed areas for the two interfering paths, and thus more sensitivity in measurements. It has been suggested [4,8,12] that measurements of the refractive index may provide the capability for determining the scattering length of an ultracold gas. As the beam velocity and temperature of the medium are reduced, the attenuation becomes very large. Because the interference experiments are sensitive to the amplitude of the transmitted wave, it is possible to perform successful experiments for high attenuation. In the experiments [1], the interfering amplitude was as low as 10^{-2}, corresponding to a transmitted intensity of 10^{-4}. Measurement of the phase shift becomes more difficult as the attenuation increases, so it is useful to know whether atom interferometry experiments would provide a practical means of determining scattering information in the ultracold limit. In this work, we investigate the attenuation and phase shift as a function of temperature and beam velocity for He, Ne, and Ar noble gases, and consider possible experiments that may be performed on these systems.

II. THEORY

The application of multiple scattering theory [13,14] to the present problem has been described previously [7]. For a dilute gas, the index of refraction is given by

$$n(k_L)=1+\frac{2\pi N}{k_L}\left\langle\frac{f(k,0)}{k}\right\rangle, \tag{1}$$

where N is the number density of the medium and k_L is the momentum of the matter wave in the laboratory frame. The forward scattering amplitude $f(k,0)$ is calculated in the center-of-mass frame for two particles with relative momentum k. The average is taken with respect to the distribution function

$$\rho(k_L,k)=\frac{m_T+m_P}{k_L}\sqrt{\frac{2\beta}{\pi m_T}}\sinh\left(\frac{\beta m_T k_L k}{\mu m_P}\right)\times\exp\left\{-\beta\left[\frac{k^2}{2\mu}\left(1+\frac{m_T}{m_P}\right)+\frac{k_L^2}{2m_P}\left(\frac{m_T}{m_P}\right)\right]\right\}, \tag{2}$$

where μ is the reduced mass $m_T m_P/(m_T+m_P)$ with m_P and m_T the respective masses of the projectile and target atoms, and β is the inverse of the Boltzmann constant times the temperature of the target gas. This distribution function takes into account different values and directions of the relative velocities [15]. The average in Eq. (1) is given by

$$\left\langle\frac{f(k,0)}{k}\right\rangle=\frac{1}{\mu}\int_0^\infty f(k,0)\rho(k_L,k)dk, \tag{3}$$

where

$$1=\int_0^\infty \rho(k_L,k)d\left(\frac{k^2}{2\mu}\right)=\frac{1}{\mu}\int_0^\infty k\rho(k_L,k)dk \tag{4}$$

normalizes the distribution function. If the target gas atoms in the medium are cooled to the limit of zero temperature, then the distribution function (2) becomes a δ function

$$\lim_{T\to 0}\rho(k_L,k)=\frac{\mu}{k}\,\delta\left(k-\frac{\mu}{m_P}k_L\right), \tag{5}$$

and

$$n(k_L)=1+\frac{2\pi m_P N}{\mu k_L^2}f\left(\frac{\mu}{m_P}k_L,0\right). \tag{6}$$

Equation (6) assumes that the medium is sufficiently dilute that a statistical coarse-graining procedure remains adequate when the de Broglie wavelength of the target atom is large. The result also applies in the $T\to 0$ limit for a mean-field description of the medium [12].

The experiments [1–3] perform simultaneous measurements of the phase shift and the attenuation of the interfering amplitude. Therefore, they are most sensitive to the ratio

$$R(k_L)=\frac{\mathrm{Re}[n(k_L)-1]}{\mathrm{Im}[n(k_L)]}=\frac{\int_0^\infty \mathrm{Re}[f(k,0)]\rho(k_L,k)dk}{\int_0^\infty \mathrm{Im}[f(k,0)]\rho(k_L,k)dk}. \tag{7}$$

The definition

$$R_0\equiv\lim_{T\to 0}R(k_L)=\frac{\mathrm{Re}\left[f\left(\frac{\mu}{m_P}k_L,0\right)\right]}{\mathrm{Im}\left[f\left(\frac{\mu}{m_P}k_L,0\right)\right]} \tag{8}$$

may be used for a matter wave traveling in an ultracold gas. The $k_L\to 0$ limit of R_0 allows a convenient determination of the parameters in the effective range expansion [8]

$$R_0(k)\sim-(a_s k)^{-1}+\tfrac{1}{2}r_e k, \tag{9}$$

where a_s is the scattering length and r_e is the effective range of the potential. The optical theorem may be used together with Eq. (9) to show that the scattering length is also given by

$$a_s=-\lim_{k\to 0}\mathrm{Re}[f(k,0)]. \tag{10}$$

The analysis given above may be generalized to include a mixture of target gas atoms [12]. The scattering amplitudes are statistically averaged by taking account of the individual gas components using the formula

$$n(k_L)=1+\frac{2\pi}{k_L}\sum_i\frac{N_i}{\mu_i}\int_0^\infty f_i(k_i,0)\rho_i(k_L,k_i)dk_i. \tag{11}$$

Equations (7) and (8) become

$$R(k_L)=\frac{\sum_i\frac{N_i}{\mu_i}\int_0^\infty \mathrm{Re}[f_i(k_i,0)]\rho(k_L,k_i)dk_i}{\sum_i\frac{N_i}{\mu_i}\int_0^\infty \mathrm{Im}[f_i(k_i,0)]\rho_i(k_L,k_i)dk_i} \tag{12}$$

and

$$R_0=\lim_{T\to 0}R(k_L)=\frac{\sum_i\frac{N_i}{\mu_i}\mathrm{Re}\left[f_i\left(\frac{\mu_i}{m_P}k_L,0\right)\right]}{\sum_i\frac{N_i}{\mu_i}\mathrm{Im}\left[f_i\left(\frac{\mu_i}{m_P}k_L,0\right)\right]}. \tag{13}$$

The scattering amplitude in the center-of-mass frame may be obtained using standard quantum partial-wave theory

$$f(k,\theta)=\frac{1}{2ik}\sum_{l=0}^{\infty}(2l+1)[\exp(2i\delta_l)-1]P_l(\cos\theta), \tag{14}$$

where δ_l is the numerically computed phase shift, and θ is the center-of-mass scattering angle. At high beam velocities, the scattering amplitude is well approximated by the eikonal approximation,

$$f(k,0)=-ik\int_0^\infty\{\exp[2i\eta(b)]-1\}b\,db, \tag{15}$$

where b is the classical impact parameter, and $\eta(b)$ is the corresponding phase-shift function

$$\eta(b)=-\frac{1}{2v}\int_{-\infty}^{+\infty}V(\sqrt{b^2+z^2})dz. \tag{16}$$

III. RESULTS

The forward-scattering amplitude is calculated from the molecular potential between the sodium and noble-gas atoms. The construction of the potentials used in this work have been described previously [7,8]. The parametrization denoted by $He^{(2)}$ in Ref. [7] was used for the Na+He potential. The Na+Ar potential produced results for the refractive index that failed to agree with a recent experiment [3] so it is worth looking at the molecular potential for this system. In Fig. 1, we show molecular curves constructed from the RKR points of three independent experimental spectra [9–11]. Table I summarizes the parameters used to obtain the RKR points. The parameters are defined by

$$G(v)=\omega_e(v+\tfrac{1}{2})-\omega_e x_e(v+\tfrac{1}{2})^2+\omega_e y_e(v+\tfrac{1}{2})^3+\omega_e z_e(v+\tfrac{1}{2})^4, \tag{17}$$

$$F_v(J)=[B_e-\alpha_e(v+\tfrac{1}{2})+\gamma_e(v+\tfrac{1}{2})^2]J(J+1), \tag{18}$$

where $G(v)$ and $F_v(J)$ are the vibrational and rotational energies, respectively. All three curves are smoothly connected to the same van der Waals expansion at $R_m=20$ a.u.

The eikonal approximation (15) and (16) was used in Ref. [3] to provide a theoretical comparison with the atom interferometry data. Because there was significant disagreement between the experimental data and the eikonal calculations, we investigated the appropriateness of the eikonal approximation. In Fig. 2, we compare results of the eikonal approximation with a numerically exact quantum treatment for the three potential curves shown in Fig. 1. The top two curves in Fig. 2 are results using the potential constructed from the

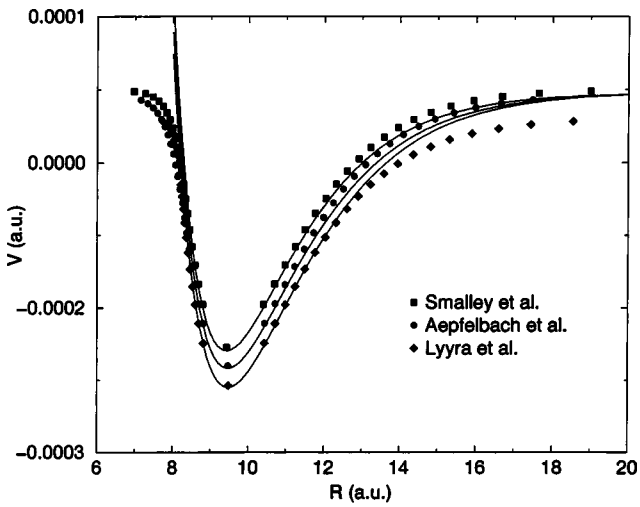

FIG. 1. Molecular potential for Na+Ar. RKR points are shown for the data of Smalley *et al.* [9], Aepfelbach, Nunnemann, and Zimmermann [10], and Lyyra *et al.* [11]. The solid curves are the potentials used in the present work. Each curve is connected smoothly to the same van der Waals expansion at 20 a.u.

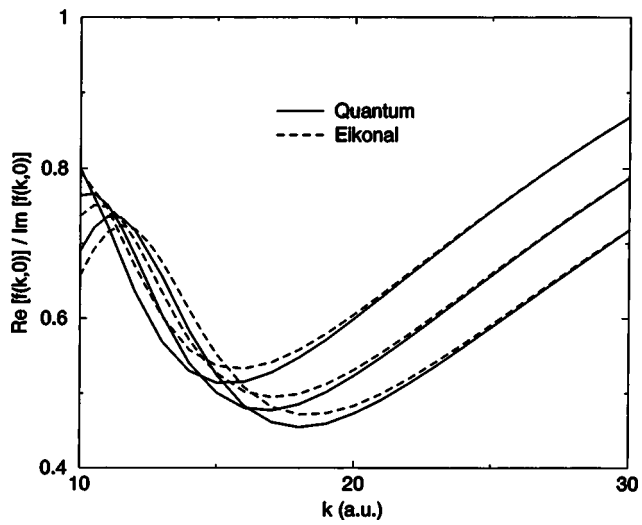

FIG. 2. Comparison of quantum calculations with eikonal calculations for the three potentials shown in Fig. 1. The top two curves are for the potential fit to the data of Smalley *et al.* [9], the middle two curves are for the potential fit to the data of Aepfelbach Nunnemann, and Zimmermann [10], and the bottom two curves are for the potential fit to the data of Lyyra *et al.* [11].

data of Smalley *et al.* [9], the middle two curves are results using the potential constructed from the data of Aepfelbach, Nunnemann, and Zimmermann [10], and the bottom two curves are results using the potential constructed from the data of Lyyra *et al.* [11]. The disagreement between the quantum and eikonal results in all three cases is not large enough to explain the disagreement between the experiment and theory presented in Ref. [3]. Figure 3 shows the ratio $\boldsymbol{R}$ versus beam velocity. The thermal average was performed using Eq. (7) at a temperature of 300 K. The theoretical curves are the results of fully converged quantum calculations and are labeled according to the data that was used to construct the potentials. The interferometry data [3] shown on the same figure is not very well reproduced by any of the theoretical calculations.

It has been suggested [4–8] that the index of refraction measurements may be useful in refining molecular potential curves. Therefore, we attempted to construct a potential for Na+Ar that provides a better fit to the interferometry data [3]. This turned out to be a difficult task. Because the potential well parameters are fairly well known, we initially constrained our adjustments to be within 5% of the accepted values given in Table I. None of the modified potentials were able to provide satisfactory agreement with the interferometry data over the entire velocity range of 500–3000 m/s. Better agreement was obtained when we allowed the harmonic frequency ω_e to be reduced by about 25% from its accepted value. Figure 4 shows theoretical results using this type of modified potential. A 25% change in ω_e is rather large considering that ω_e differs by at most 2.6% for the three independent experiments [9–11]. Even with the 25% adjustment, it was not possible to obtain satisfactory agreement at high velocities (see Fig. 4). It was argued [3] that a

TABLE I. Potential parameters for Na+Ar.

Parameter	Ref. [9]	Ref. [10]	Ref. [11]	Modified [9]
R_e (Å)	4.991	5.008	5.011	4.991
D_e (cm^{-1})	38.9	41.7	44.7	37
ω_e (cm^{-1})	13.66	13.313	13.358	10
$\omega_e x_e$ (cm^{-1})	1.2	0.994	1.038	0
$\omega_e y_e$ (cm^{-1})	0	−0.029	−0.0111	0
$\omega_e z_e$ (cm^{-1})	0	0.0024	0	0
B_e (cm^{-1})	0.046 37	0.046 08	0.045 99	0.046 37
α_e (cm^{-1})	−0.003 856	−0.0034	−0.0032	0
γ_e (cm^{-1})	0	0	−.000 28	0
R_m (a.u.)	20	20	20	20
C_6 (a.u.)	190	190	190	190
C_8 (a.u.)	12 700	12 700	12 700	12 700
C_{10} (a.u.)	820 000	820 000	820 000	820 000

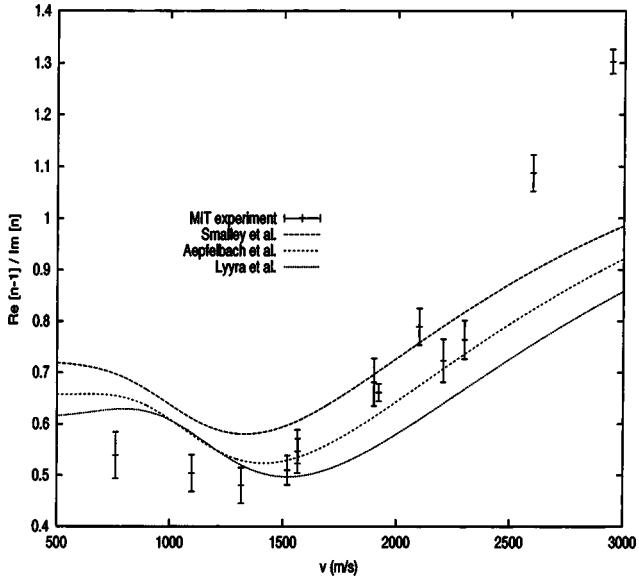

FIG. 3. Ratio versus beam velocity. The thermal average was done at 300 K. The theoretical curves are labeled according to the experimental data used to construct the molecular potentials.

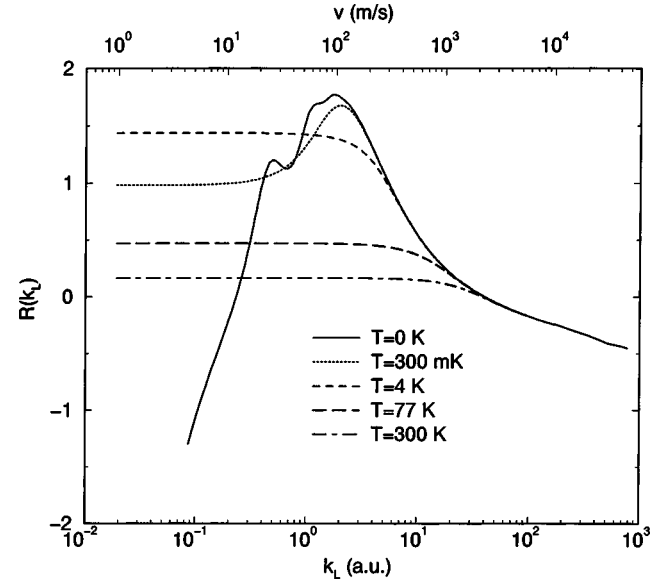

FIG. 5. Ratio $R(k_L)$ for Na+^{3}He. The results for several temperatures are shown along with the laboratory wave number and beam velocity.

poor understanding of the connecting region between the short- and long-range parts of the potential may be responsible for the lack of agreement between theory and experiment. We explored many different types of interpolation in this connecting region, but were unable to find a physically reasonable curve that successfully reproduced the interferometry data [3]. Further investigation is certainly needed to establish the correct form of the potential in this region.

It would seem that the disagreement between theory and experiment described above should be resolved before attempting to understand the behavior at cold and ultracold temperatures. It is interesting to consider, however, the qualitative features that enter into the analysis as the temperature and beam velocities are reduced. Figures 5–7 show the ratio $R(k_L)$ for Na atoms passing through a gas of ^{3}He, Ne, and Ar. The results for several temperatures are shown along with the laboratory wave number and beam velocity. We assumed temperatures that are achievable using liquid nitrogen, liquid helium, and helium buffer gas cooling methods [16]. Room temperature and the $T \rightarrow 0$ limit are shown for comparison. The number of bound states supported by the molecular potentials may be found by counting the number of maxima in R_0 (excluding resonances). In Fig. 5, we see mostly smooth behavior as a function of wave number. Be-

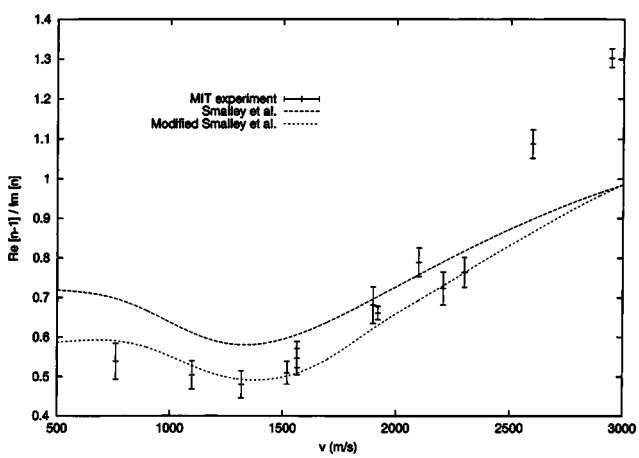

FIG. 4. Results for Na+Ar at 300 K. The long-dashed curve was obtained using a Morse potential with parameters from Smalley *et al.* [9]. The short-dashed curve was obtained using a 5% modification to the dissociation energy and a 25% modification to the harmonic frequency (see Table I). The equilibrium separation was the same in both cases and the potentials were matched to the van der Waals expansion at 20 a.u.

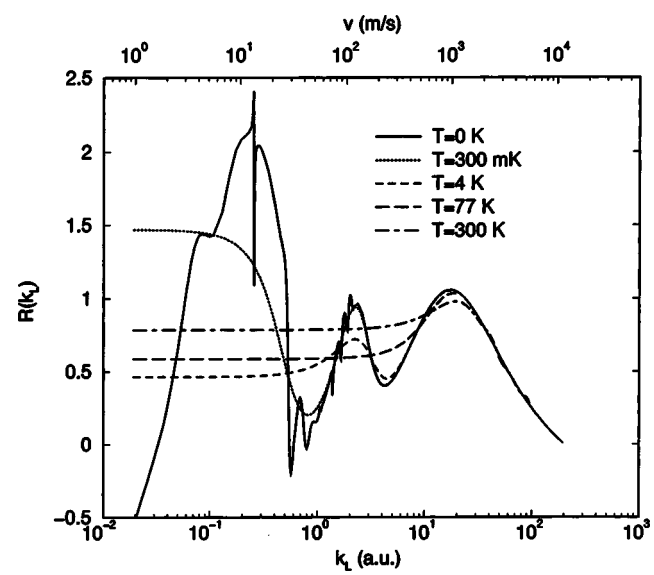

FIG. 6. Ratio $R(k_L)$ for Na+Ne. The results for several temperatures are shown along with the laboratory wave number and beam velocity.

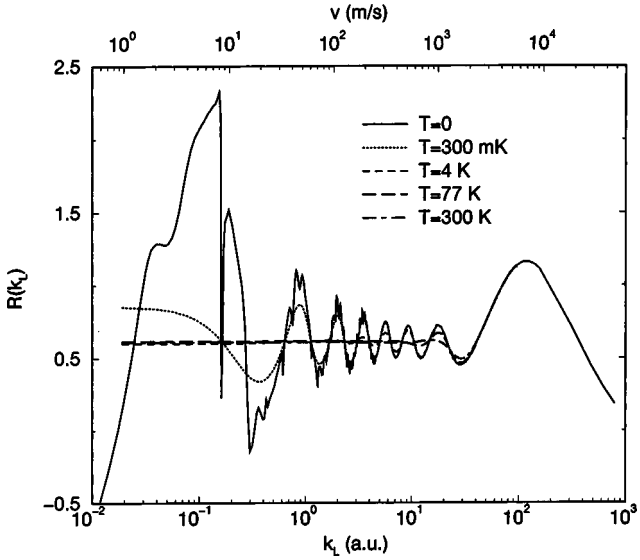

FIG. 7. Ratio $R(k_L)$ for Na+Ar. The results for several temperatures are shown along with the laboratory wave number and beam velocity. The molecular potential constructed from the data of Lyyra *et al.* [11] was used in the calculations.

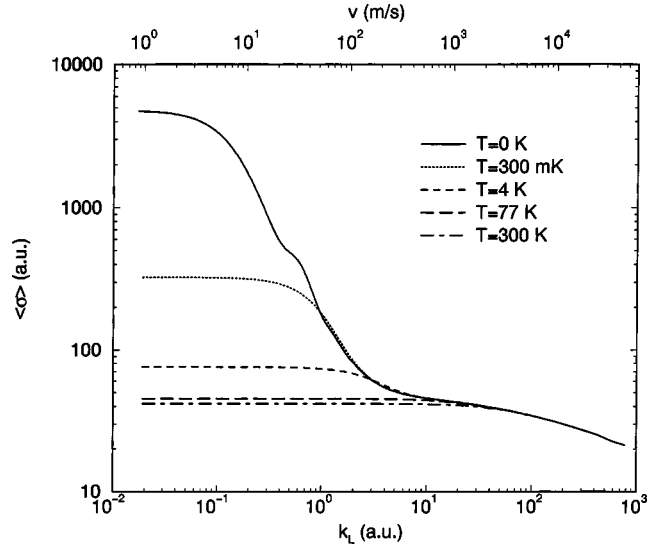

FIG. 8. Average cross section $\langle\sigma\rangle$ for Na+ ^{3}He. The results for several temperatures are shown along with the laboratory wave number and beam velocity.

cause the Na-He potential has only one weakly bound state, there is only one glory oscillation and perhaps a weak shape resonance. Figures 6 and 7 show more interesting behavior. Glory oscillations and scattering resonances are clearly evident in these curves for $T\rightarrow 0$. The limiting $k_L\rightarrow 0$ behavior is different for $T=0$ than for finite temperatures. This is due to $\rho(k_L,k)$ which reduces to Eq. (5) when $T\rightarrow 0$ and to a Maxwellian distribution when $k_L\rightarrow 0$. The resonant structure begins to disappear around 10 mK. As the temperature is increased to 300 mK, the glory oscillations remain, but the resonant structure is not resolved. At 4 K, about half of the glory oscillations are resolved. Only the last glory oscillation is resolved at room temperature.

The amplitude of the matter wave decreases exponentially as it travels through the medium according to

$$A(x)=\exp\left(-2\pi N\,\mathrm{Im}\left\langle\frac{f(k,0)}{k}\right\rangle x\right)=\exp(-\tfrac{1}{2}N\langle\sigma\rangle x), \tag{19}$$

where x is the distance traveled and σ is the total scattering cross section. Figures 8–10 show cross sections for Na atoms scattering from ^{3}He, Ne, and Ar averaged with respect to the distribution function (2). The cross section increases dramatically as the temperature of the medium is decreased. As the beam velocity approaches zero, the cross sections reach a constant value in accordance with Wigner's threshold law. The figures show that the averaged cross section in the limit of zero temperature and beam velocity is typically equal to one hundred times the room temperature value. Therefore, for a given density and distance traveled, the attenuation at ultracold temperatures would be equal to the attenuation at room temperature taken to the 100th power. A more realistic estimate may be made by recognizing that the number density at cold temperatures would be less than at room temperature. This provides a decreasing contribution to the argument of the exponential in Eq. (19) that would oppose the increasing contribution coming from the cross section.

Measurements of $R(k_L)$ and $\langle\sigma\rangle$ allow a determination of the phase shift of the matter wave, which is proportional to

TABLE II. Effective range parameters.

Target gas	a_s (a.u.)	r_e (a.u.)	Bound states
^{3}He	70	21	1
Ne	144	40	3
Ar	170	60	8

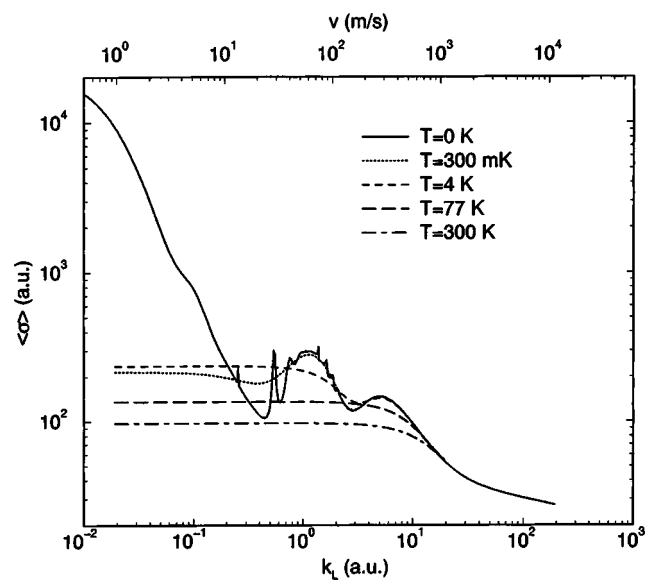

FIG. 9. Average cross section $\langle\sigma\rangle$ for Na+Ne. The results for several temperatures are shown along with the laboratory wave number and beam velocity.

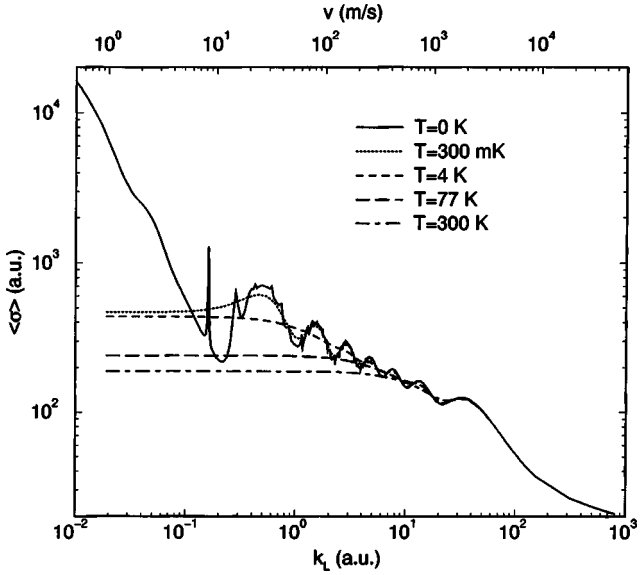

FIG. 10. Average cross section $\langle\sigma\rangle$ for Na+Ar. The results for several temperatures are shown along with the laboratory wave number and beam velocity. The molecular potential constructed from the data of Lyyra *et al.* [11] was used in the calculations.

$$\phi = \mathrm{Re}\left\langle \frac{f(k,0)}{k} \right\rangle. \tag{20}$$

Figures 11–13 show ϕ as a function of wave number, beam velocity, and temperature for Na atoms scattering from ^{3}He, Ne, and Ar. Similar to the attenuation, the phase shift increases significantly as the temperature of the medium is decreased. As the beam velocity approaches zero, the phase shift reaches a constant value for finite temperatures. At $T=0$, however, the situation is very different. From Eq. (10), we see that the real part of $f(k,0)$ approaches a constant scattering length and that ϕ diverges as k^{-1}. Table I gives the scattering lengths and effective ranges for the potentials used in this work.

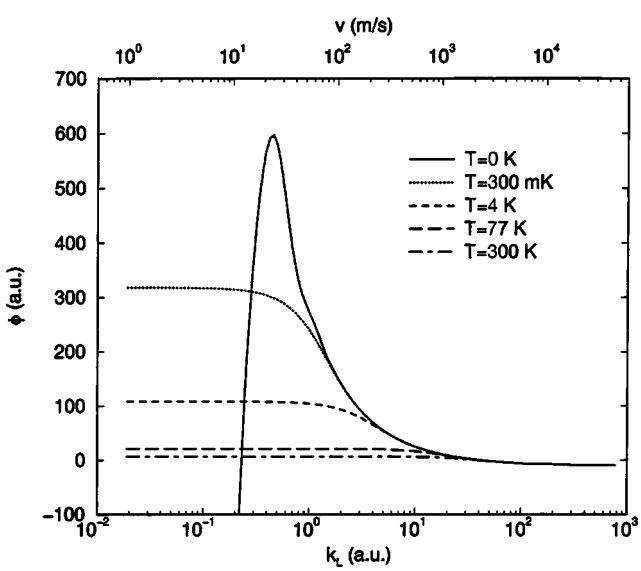

FIG. 11. Real part of $\langle f(k,0)/k\rangle$ for Na+^{3}He. The results for several temperatures are shown along with the laboratory wave number and beam velocity.

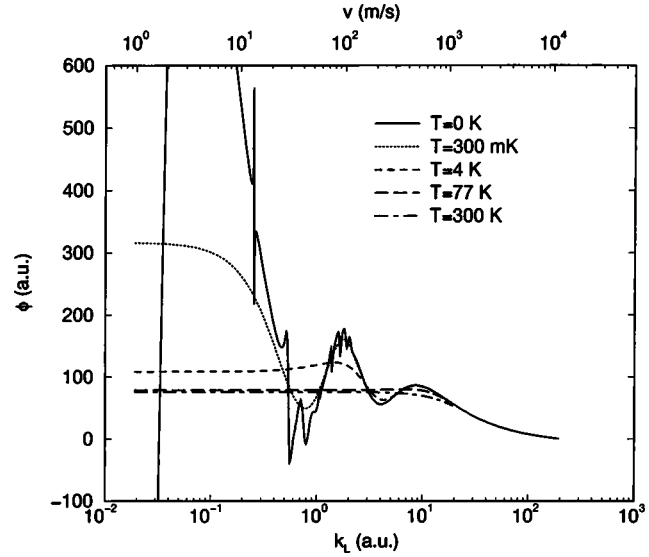

FIG. 12. Real part of $\langle f(k,0)/k\rangle$ for Na+Ne. The results for several temperatures are shown along with the laboratory wave number and beam velocity.

IV. CONCLUSIONS

We have calculated the index of refraction for a sodium atom matter wave as a function of temperature and beam velocity. Resonances and glory oscillations are present in the center-of-mass scattering amplitude. However, it would be necessary to significantly cool the noble-gas medium in order to resolve the resonances and all but one of the oscillations in the index of refraction. One possibility would be to

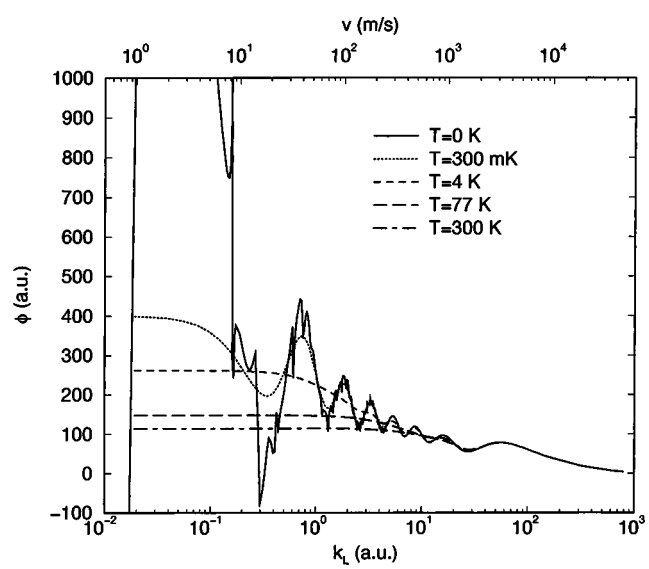

FIG. 13. Real part of $\langle f(k,0)/k\rangle$ for Na+Ar. The results for several temperatures are shown along with the laboratory wave number and beam velocity. The molecular potential constructed from the data of Lyyra *et al.* [11] was used in the calculations.

use helium buffer gas cooling [16]. The index of refraction could be determined for a noble gas in isolation or in a mixture with a helium buffer gas. The contribution to the refractive index coming from the helium gas would be smoothly varying, whereas the contribution coming from an argon or neon gas would reveal oscillatory behavior arising from glory scattering. The resonant structure would still not be detectable at the temperatures that are achievable using buffer gas cooling. At ultracold temperatures and beam velocities, the attenuation of the matter wave is extremely large. Therefore, an intense source of matter waves such as the sodium atom laser [17] may be needed in order to build up a detectable interference pattern.

ACKNOWLEDGMENTS

We would like to thank David Pritchard and members of the MIT atom interferometry group for helpful communications and for providing us with the experimental data used in this work. We also thank Alex Dalgarno and Vasili Kharchenko for helpful conversations. This work was funded by the National Science Foundation, Grant No. PHY-0070920.

[1] J. Schmiedmayer, M. S. Chapman, C. R. Ekstrom, T. D. Hammond, S. T. Wehinger, and D. E. Pritchard, Phys. Rev. Lett. **74**, 1043 (1995).

[2] *Atom Interferometry*, edited by P. R. Berman (Academic, New York, 1997).

[3] T. D. Roberts, A. D. Cronin, D. A. Kokorowski, and D. E. Pritchard Phys. Rev. Lett. **89**, 200406 (2002).

[4] J. Vigue, Phys. Rev. A **52**, 3973 (1995).

[5] E. Audouard, P. Duplaa, and J. Vigue, Europhys. Lett. **32**, 397 (1995).

[6] C. Champenois, E. Audouard, P. Duplaa, and J. Vigue, J. Phys. II **7**, 523 (1997).

[7] R. C. Forrey, L. You, V. Kharchenko, and A. Dalgarno, Phys. Rev. A **54**, 2180 (1996).

[8] R. C. Forrey, L. You, V. Kharchenko, and A. Dalgarno, Phys. Rev. A **55**, R3311 (1997).

[9] R. E. Smalley, D. A. Auerbach, P. S. H. Fitch, D. H. Levy, and L. Wharton, J. Chem. Phys. **66**, 3778 (1977).

[10] G. Aepfelbach, A. Nunnemann, and D. Zimmermann, Chem. Phys. Lett. **96**, 311 (1983).

[11] A. M. Lyyra, W. P. Lapatovich, P. E. Moskowitz, M. D. Havey, R. Ahmed-Bitar, R. A. Gottscho, and D. E. Pritchard (unpublished).

[12] V. Kharchenko and A. Dalgarno, Phys. Rev. A **63**, 023615 (2001).

[13] M. Lax, Rev. Mod. Phys. **23**, 287 (1951).

[14] V. F. Sears, Phys. Rep. **82**, 1 (1982).

[15] This point has caused some confusion in the literature. For clarification, see R. C. Forrey, V. Kharchenko, and A. Dalgarno, J. Phys. B **35**, L261 (2002).

[16] J. D. Weinstein, R. deCarvalho, T. Guillet, B. Friedrich, and J. M. Doyle, Nature (London) **395**, 148 (1998).

[17] S. Inouye, T. Pfau, S. Gupta, A. P. Chikkatur, A. Görlitz, D. E. Pritchard, and W. Ketterle, Nature (London) **402**, 641 (1999).